SIAM J. Appl. Math.
Vol. 0, No. 0, pp. 000–000

NEURAL TIMING IN HIGHLY CONVERGENT SYSTEMS*

COLLEEN MITCHELL† AND MICHAEL REED‡

Abstract. In order to study how the convergence of many variable neurons on a single target can sharpen timing information, we investigate the limit as the number of input neurons and the number of incoming spikes required to fire the target both get large with the ratio fixed. We prove that the standard deviation of the firing time of the target cell goes to zero in this limit, and we derive the asymptotic forms of the density and the standard deviation near the limit. We use the theorems to understand the behavior of octopus cells in the mammalian cochlear nucleus.

Key words. neural networks, precision, timing, convergence, octopus cells

AMS subject classifications. 92, 60

DOI. 10.1137/07068775X

1. Introduction.

A fundamental question in neurobiology is to understand how the central nervous system (CNS) can perform accurate and reliable calculations with neurons that are intrinsically variable and unreliable devices. Three more concrete versions of the question have received much attention: (1) How can network and/or cellular properties sharpen timing information or create accurate coincidence detectors? (2) How can synchronous activity in large groups of neurons be created and maintained? (3) Under what circumstances can intrinsic noise improve information processing capabilities?

The first question has long been studied in the auditory brainstem because it is experimentally accessible and because cellular, behavioral, and psychoacoustic experiments show that the auditory system can make extremely fine timing distinctions in the microsecond (or even nanosecond) range, even though individual neurons in the auditory nerve (AN) show latency standard deviations of approximately one millisecond in repeated trials with the same sound [25, 10, 45, 33, 50]. Lord Rayleigh [34] first proposed that the auditory system uses binaural timing distinctions to localize sound, and Jeffress [21] proposed the first neural mechanism based on delay lines and coincidence detection. Colburn [8] clearly formulated the question of how the auditory system can detect small time differences, given the noise in the AN, and went on to create some of the first mathematical models [9]. Important experimental studies include those of Rhode and Smith [37, 38] and Goldberg and Brown [14].

All fibers of the AN synapse on cells of the cochlear nucleus (CN). There are many different cell types in the CN that receive different numbers of AN synapses and have different response properties. Two experimental properties have received continuing attention from experimentalists and modelers. First, several CN cell types show "onset" responses; that is, they fire a single spike shortly after the initiation of the sound; the time lag is called the latency. The standard deviation of latency in AN fibers under repeated trials is of the order of 1 msec, but the standard deviation

*Received by the editors May 22, 2006; accepted for publication (in revised form) April 11, 2007; published electronically DATE. The research in this paper and its preparation were supported by NSF grants DMS-0109872 and DMS-0616710.
http://www.siam.org/journals/siap/x-x/66050.html
†Department of Mathematics, University of Iowa, 14 MacLean Hall, Iowa City, IA 52242-1419 (colleen-mitchell@uiowa.edu).
‡Department of Mathematics, Duke University, Science Drive, Durham, NC 27708 (reed@duke.math.edu).

of latency in some onset units of the CN is as much as an order of magnitude lower. Second, AN fibers phase lock to low frequency sounds, and this phase locking is even better in some CN units. Burkitt and Clark [4, 5] use numerical simulations of leaky integrate-and-fire models to study how convergence of inputs effects both the onset response and the increase in synchrony seen in target cells. Kalluri and Delgutte [23, 24] have created a computational model using leaky integrate-and-fire for the CN target cells and an adaptively filtered Poisson processes to model spike trains along each of the convergent AN fibers. They are interested in determining what properties of the target cell, the filtered Poisson process in AN fibers, the convergence from AN fibers to the target, and adaptation in the hair cells cause the target neuron to have an onset response with low spontaneous rate. Young, Rothman, and coworkers [51, 39, 40, 41, 42, 43] have conducted experiments and used numerical simulations of biophysical models to investigate how the response properties of CN neurons depend on the details of their channel kinetics. Similarly, Cai, Walsh, and McGee [6, 7] used simulations of biophysical models to investigate the onset response of octopus cells in the CN using the physiological properties discovered by Oertel and coworkers [15, 13, 32].

The overall goal of this computational modeling was to investigate how convergence, detailed biophysics of CN neurons, and the known properties of auditory spike trains give rise to onset responses, higher synchrony, and the sharpening of timing in CN neurons. Their numerical computations suggest strongly that there is a connection between the amount of convergence and the sharpening of timing information. However, their models are so elaborate and have so many parameters that it is difficult to make precise the mechanisms by which convergence sharpens timing. For this reason, we have been studying the much simpler model described below in which convergence and the sharpening of timing are isolated as the objects of study. The simplicity of the model allows us to use the tools of probability theory and mathematical statistics to prove theorems that make precise the relationship between convergence and the sharpening of timing. Their numerical modeling and our theorems contribute not only to understanding the auditory brainstem but also address question (1) and by implication question (2) if several of these systems are connected in series. In other auditory brainstem work, Svirskis et al. [48] investigate through experiment and biophysical modeling the properties of medial superior olive neurons that make them excellent coincidence detectors and propose that coincidence detection is improved in some circumstances by a noisy background. Thus their work relates directly to the ideas of stochastic resonance in neural systems put forward by Greenwood et al. [17] and Stemmler [47] and so addresses question (3).

In our simple convergence model, there are n identical input neurons, and all receive the same stimulus. Each fires a single action potential at a time selected independently from a probability density f with standard deviation 1 msec. The axons of the n neurons are of equal length and project to one target neuron that fires a single action potential the first time that it has received m inputs in the previous ε msec. Of course, the target neuron may not fire at all in response to a particular stimulus. We denote the conditional density of the time of firing of the target neuron, given that it fires, by $g_{n,m,\varepsilon,f}$ and its standard deviation by $\sigma_{n,m,\varepsilon,f}$, since both will depend on n, m, ε, and f. If $\sigma_{n,m,\varepsilon,f} < 1$ msec, then we say that timing has been sharpened. A change of variables shows that there is a scaling law $\sigma_{n,m,\varepsilon,f} = s\sigma_{n,m,\frac{\varepsilon}{s},f_s}$, where $f_s(t) \equiv sf(st)$, so there is no loss in generality in taking the standard deviation of the input density f to be 1 msec [35, 29].

Although the formulation of the problem is simple, it is difficult or impossible to derive closed form expressions for $g_{n,m,\varepsilon,f}$ and $\sigma_{n,m,\varepsilon,f}$ except in very special cases.

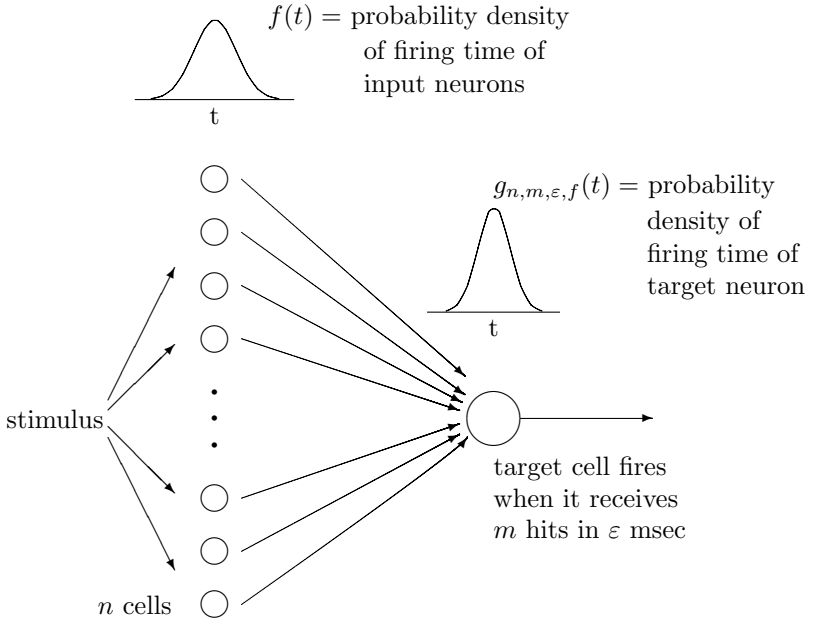

FIG. 1. *The basic model. The target cell receives n independently and identically distributed inputs and fires the first time it receives m within ε msec.*

Additionally, Monte Carlo simulations [35] show that, for n and f fixed, $\sigma_{n,m,\varepsilon,f}$ can have surprisingly complicated behavior as a function of m, the numbers of hits required, and ε, the size of the time window. For example, even for simple choices of f (uniform, exponential, normal) and $n = 10$, $\sigma_{n,m,\varepsilon,f}$ is sometimes monotone and sometimes nonmonotone as a function of either m or ε with the other held fixed. In these circumstances, it is natural to ask whether the behavior of $\sigma_{n,m,\varepsilon,f}$ is simpler in certain asymptotic limits. As $\varepsilon \to \infty$, the neuron will surely fire at the time of the mth hit, so $\sigma_{n,m,\infty,f}$ is given by order statistics, which is well understood. In the literature this model is called the (nonleaky) integrate-and-fire model. It is used by Marsalek, Koch, and Maunsell [27], it is the simplest model used by Burkitt and Clark [4], and it is the "analytic coincidence detector model" of Kalluri and Delgutte [23]. Thus those models are a special case of our model. Mitchell [29, 30] considered the singular asymptotic limit $\varepsilon \to 0$, proved that

$$g_{n,m,\varepsilon,f} \to \frac{f^m}{\int f^m} \tag{1}$$

independent of n, and derived an asymptotic form for $g_{n,m,\varepsilon,f}$ and $\sigma_{n,m,\varepsilon,f}$ near the limit.

In this paper, we study the limit as $n \to \infty$, $m \to \infty$ with the ratio $\frac{m}{n}$ held fixed. There are good theoretical and experimental reasons to think that this limit is important. First, it is relatively easy to see (Theorem 2.1 below), under reasonable hypotheses on f, that $\sigma_{n,m,\varepsilon,f} \to 0$ as $n \to \infty$ with m held fixed. That is, one can sharpen up timing as much as one wants by assuming a model with n large, for example by choosing $m = 1$, in which case the target always fires at first hit. Young, Robert, and Schofner [51] already pointed out that if f is exponential and $m = 1$, then $\sigma_{n,1,\varepsilon,f} = \frac{1}{n}$. The trouble is that many neurons (in particular those in the auditory

nerve) have high spontaneous firing rates, and so with high n and low m the target cell will have a high spontaneous rate, which ruins its role as a neuron that measures the time since the stimulus. Thus it is natural to ask whether taking both n *and* m large can produce a system that sharpens timing dramatically but also has a very low spontaneous rate. The approximate calculations of Burkitt and Clark [4] and the numerical simulations of Kalluri and Delgutte [23] suggest strongly that there should be a clean asymptotic limit as $n \to \infty$ with $\frac{m}{n}$ held fixed. Furthermore, there is good reason to think that octopus cells in the cochlear nucleus operate near this asymptotic limit. Oertel [32] has found that the octopus cells receive up to 100 inputs from AN fibers and that between 20 and 50 hits within a small time window are required to make them fire.

In section 2, we answer the above question by showing that $\sigma_{n,m,\varepsilon,f} \to 0$ as $n \to \infty$, $m \to \infty$, with $\frac{m}{n}$ fixed. In section 3, we derive the asymptotic forms of $g_{n,m,\varepsilon,f}$ and $\sigma_{n,m,\varepsilon,f}$ near the limit. And in section 4, we apply the results to octopus cells.

2. Limit theorems as $n \to \infty$. Let $\{X_i\}_{i=1}^n$ denote the n independently and identically distributed random variables for the firing times of the inputs. Assume that the X_i's have density $f(x)$, continuous distribution $F(x)$, and finite mean and standard deviation. We will use T_n to denote the random variable for the firing time of the output (a formal definition is given in (6)). For some of the results below we also assume that there is an x_o so that

$$\int_{-\infty}^{x_o} f(x)\,dx = 0 \quad \text{and} \quad \int_{x_o}^{x+a} f(x)\,dx \ > 0 \quad \text{for all } \ a > 0. \tag{2}$$

This is reasonable biologically since the input neurons cannot respond before the stimulus (and perhaps not for some fixed delay afterwards).

We first consider the case where $n \to \infty$ while m and ε are fixed.

THEOREM 2.1. *Let f be a given probability density satisfying* (2), *and let $0 < \varepsilon \le \infty$ and m be fixed. Then, as $n \to \infty$, the following hold*:

(i) *The probability that the target cell fires $\longrightarrow 1$.*

(ii) *$g_{n,m,\varepsilon,f} \longrightarrow \delta_{x_o}$; that is, $T_n \longrightarrow T$ in distribution. Further, T_n converges in probability to the point mass at x_o.*

(iii) *If f has compact support, then $\sigma_{n,m,\varepsilon,f} \longrightarrow 0$.*

Proof. Let $a > 0$ be given, and define $\gamma \equiv \int_{x_o}^{x_o+a} f(x)\,dx \ > 0$. Let Y_i be the random variable with value 1 if $x_o \le X_i \le x_o + a$ and zero otherwise. Then, for each k,

$$P\left\{\sum_{i=1}^n Y_i = k\right\} \ = \ \gamma^k(1-\gamma)^{n-k}\binom{n}{k},$$

so that

$$P\left\{\sum_{i=1}^n Y_i < m\right\} = \sum_{k=0}^{m-1} \gamma^k(1-\gamma)^{n-k}\binom{n}{k} \ \le \ C\beta^n, \tag{3}$$

where β satisfies $1-\gamma < \beta < 1$. The constants β and C depend on m and γ but not on n, and so

$$P\left\{\sum_{i=1}^n Y_i \ge m\right\} \to 1 \quad \text{as } \ n \to \infty. \tag{4}$$

Let S denote the event that the target cell fires and T_n be the time of firing. If we choose $a = \varepsilon$, then

$$P\{S\} \;\geq\; P\{S \cap \{x_o \leq T_n \leq x_o + \varepsilon\}\} \;=\; P\{\textstyle\sum_{i=1}^{n} Y_i \geq m\},$$

so (i) follows from (4). For all $0 < a \leq \varepsilon$,

$$P\{\{x_o \leq T_n \leq x_o + a\}|S\} = P\{S \cap \{x_o \leq T_n \leq x_o + a\}\}/P\{S\} \quad \to 1 \tag{5}$$

as $n \to \infty$, which proves (ii).

To prove (iii) without assuming compact support, we would need to prove a uniform integrability condition. We will prove such a condition in the case of the main theorem of this section (Theorem 2.3) but omit it here. If we assume that f does have compact support, which is a reasonable hypothesis from a biological perspective, then it is easy to check that $E(T_n|S) \to x_o$ and $E(T_n^2|S) \to x_o^2$ as $n \to \infty$, which gives (iii).

Theorem 2.1 shows, as expected, that if it takes a fixed number of hits in an ε time window to fire the target cell, then one can achieve any improvement in accuracy one wants by taking n large enough. This confirms the general belief in the literature [51, 4, 23] that greater convergence sharpens timing information. However, notice the important hypothesis that m is held fixed. Example 2.1 shows that if m is not fixed, then increasing convergence may make timing worse. Example 2.2 shows that, given a firing mechanism at the target cell, the answer to the question of whether timing gets better of worse depends on f. Thus one should be very careful about drawing general conclusions from simulations, since the results may depend on the form chosen for the noise.

Example 2.1. If $m = n$, $\varepsilon = \infty$, and f is exponential, the standard deviation of the firing times is monotone increasing. This is because the cell will fire when the last (n^{th}) hit arrives. For large n this will be somewhere out in the tail of the distribution. See Table 1 for values. The final entry is computed using the asymptotic behavior of the n^{th} order statistic [44]. Note that this case is not covered by Theorem 2.2 below because $\varepsilon = \infty$. It is also not covered by Theorem 2.3 below because the set $\{x \,|\, F(x) - F(x - \varepsilon) \geq \frac{m}{n}\}$ is empty.

Example 2.2. If $m = n$, $\varepsilon = \infty$, and f is uniform, the standard deviation of the firing times is monotone decreasing. This is because the nth hit out of n will be likely

TABLE 1
Values of σ for different n.

n	Exponential	Uniform
1	1.000 msec	1.000 msec
2	1.118 msec	0.816 msec
3	1.166 msec	0.671 msec
4	1.193 msec	0.566 msec
5	1.210 msec	0.488 msec
6	1.221 msec	0.429 msec
7	1.230 msec	0.382 msec
8	1.236 msec	0.344 msec
9	1.241 msec	0.313 msec
10	1.245 msec	0.287 msec
15	1.257 msec	0.203 msec
20	1.263 msec	0.157 msec
30	1.270 msec	0.108 msec
∞	1.283 msec	0.000 msec

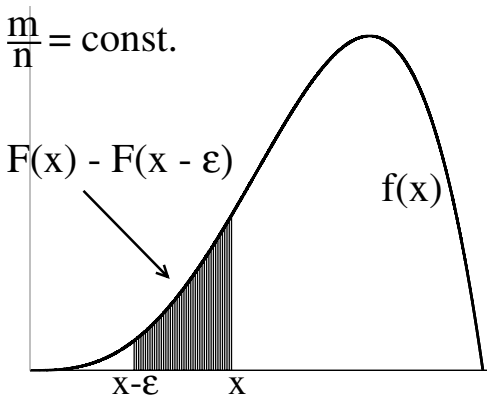

FIG. 2. *An example density to illustrate the derivation of T. T is the smallest value for x so that the area under the density curve between $x - \varepsilon$ and x is at least $\frac{m}{n}$.*

to be close to the right edge of the distribution. Note that this case is not covered by Theorem 2.2 below because $\{x \,|\, F(x) - F(x-\varepsilon) \geq \frac{m}{n}\}$ is not empty. It is also not covered by Theorem 2.3 below because $F(x) - F(x-\varepsilon)$ is not increasing at T.

We now consider the more interesting case where $n \to \infty$ with $\frac{m}{n}$ fixed. To see the intuition, consider the particular f depicted in Figure 2. For any x, we expect that approximately the fraction $F(x) - F(x-\varepsilon)$ of n selections from f should lie in the interval $[x-\varepsilon, x]$. Thus if $F(x) - F(x-\varepsilon) \geq \frac{m}{n}$, we expect that m or more selections will lie in $[x-\varepsilon, x]$, and thus x is certainly a candidate for the firing time of the target cell. Recall that the cell fires the *first* time that it gets m hits in an ε interval. Therefore, we define

$$T \;=\; \inf_x \left\{ x \,|\, F(x) - F(x-\varepsilon) \geq \frac{m}{n} \right\}$$

and expect that for large n the firing time should be close to T. Of course, depending on f, there may be no points in the set $\{x \,|\, F(x) - F(x-\varepsilon) \geq \frac{m}{n}\}$.

For the proofs below, we need to introduce some machinery. For each set of n independent selections, $\{X_i\}_{i=1}^n$, from f, we consider the *sample distribution function*

$$F_n(x) \;\equiv\; \frac{1}{n} \sum_{i=1}^{n} I(X_i \leq x),$$

where I is the indicator function taking value 1 if $X_i \leq x$ and 0 otherwise. We can now define the random variable for the output firing time T_n in terms of F_n. Choose any $M > T$, and define the random variable T_n to be

$$T_n \;=\; \inf_x \left\{ x \,|\, F_n(x) - F_n(x-\varepsilon) \geq \frac{m}{n} \right\} \tag{6}$$

if the set is non empty and $T_n = M$ otherwise.

For n large it is known that $F_n(x)$ is a good approximation to $F(x)$. This is expressed via the *Kolmogorov–Smirnov distance*,

$$D_n \;\equiv\; \sup_{-\infty < x < \infty} |F_n(x) - F(x)|.$$

The classical Glivenko–Cantelli lemma (for a proof, see [2]) states that $D_n \to 0$ with probability one.

THEOREM 2.2. *Suppose that* $0 < \varepsilon < \infty$ *and* $0 < \frac{m}{n} \leq 1$ *are fixed and that the set* $\{x \,|\, F(x) - F(x-\varepsilon) \geq \frac{m}{n}\}$ *is empty. Then the probability that the target cell fires converges to zero as* $n \to \infty$.

Proof. Since F is continuous and $\{x \,|\, F(x) - F(x-\varepsilon) \geq \frac{m}{n}\}$ is empty, there exists $\alpha > 0$ so that

$$F(x) - F(x-\varepsilon) \;\leq\; \frac{m}{n} - \alpha \quad \text{for all } x.$$

Therefore,

$$\begin{aligned} P\{\text{target cell fires}\} &= P\{\text{ at least } m \text{ hits in } [x-\varepsilon, x] \text{ for some } x\} \\ &= P\{\text{ at least } m \text{ hits in } (x-\varepsilon, x] \text{ for some } x\} \\ &= P\left\{F_n(x) - F_n(x-\varepsilon) \geq \frac{m}{n} \text{ for some } x\right\} \\ &\leq P\{F_n(x) - F(x) + F(x-\varepsilon) - F_n(x-\varepsilon) \geq \alpha) \text{ for some } x\} \\ &\leq P\{2D_n \geq \alpha)\}, \end{aligned}$$

which converges to zero by the Glivenko–Cantelli lemma. Thus, the probability that the target cell fires goes to zero as $n \to \infty$.

THEOREM 2.3. *Suppose that the set* $\{x \,|\, F(x) - F(x-\varepsilon) \geq \frac{m}{n}\}$ *is nonempty, and define* T *as above. Suppose that* $F(x) - F(x-\varepsilon)$ *is strictly increasing at* T *and that* $0 < \varepsilon \leq \infty$ *and the ratio* $0 < \frac{m}{n} \leq 1$ *are fixed. Then, as* $n \to \infty$, *the following hold*:

(i) *The probability that the target cell fires* $\longrightarrow 1$.

(ii) $g_{n,m,\varepsilon,f} \longrightarrow \delta_T$; *that is,* $T_n \longrightarrow T$ *in distribution. Further,* T_n *converges to the point mass at* T *with probability one.*

(iii) $\sigma_{n,m,\varepsilon,f} \longrightarrow 0$.

Proof. To prove (i), note that, by the strict monotonicity at T, the set $\{x \mid F(x) - F(x-\varepsilon) \geq \frac{m}{n}\}$ is nonempty. Note that here we have used only that the set is not empty, but we use the stronger monotonicity hypothesis for the proof of (ii). Thus, there is an $\bar{x}$ so that $F(\bar{x}) - F(\bar{x}-\varepsilon) \equiv \gamma > \frac{m}{n}$. Let Y_i be the random variable that has value 1 if X_i is in $[\bar{x}-\varepsilon, \bar{x}]$ and 0 otherwise. The Y_i are independent Bernoulli random variables with mean γ. Thus,

$$\begin{aligned} P\{Y_1 + \cdots + Y_n < m\} \;&=\; P\left\{\frac{Y_1 + \cdots + Y_n}{n} - \gamma < \frac{m}{n} - \gamma\right\} \\ &\longrightarrow 0 \end{aligned}$$

as $n \to \infty$ by the weak law of large numbers. If there are m or more of the X_i in the particular interval $[\bar{x}-\varepsilon, \bar{x}]$, the target cell fires, and so (i) is proved.

To prove (ii), let $0 < \mu < M - T$ be given, where M is the constant from the definition of T_n (6). We note that the continuity of F and the fact that $F(x) \to 0$ as $x \to -\infty$ imply that there is an $\alpha > 0$ so that

$$\sup_{x < T-\mu} (F(x) - F(x-\varepsilon)) < \frac{m}{n} \;-\; \alpha. \tag{7}$$

Further, by the continuity of F and monotonicity at T, there is a $\beta > 0$ so that

$$\sup_{x < T+\mu} (F(x) - F(x-\varepsilon)) > \frac{m}{n} \;+\; \beta. \tag{8}$$

We will show that $P\{|T_n - T| > \mu\} \to 0$ as $n \to \infty$. First,

$$\begin{aligned} P\{T_n < T - \mu\} &= P\left\{\exists x < T - \mu \,|\, F_n(x) - F_n(x-\varepsilon) \geq \frac{m}{n}\right\} \\ &\leq P\{\exists x < T - \mu \,|\, F_n(x) - F_n(x-\varepsilon) - (F(x) - F(x-\varepsilon)) \geq \alpha\} \\ &\leq P\{2D_n > \alpha\}. \end{aligned}$$

Similarly,

$$\begin{aligned} P\{T_n > T + \mu\} &= P\left\{F_n(x) - F_n(x-\varepsilon) < \frac{m}{n} \ \ \forall x < T + \mu\right\} \\ &\leq P\{F(x) - F(x-\varepsilon) - F_n(x) + F_n(x-\varepsilon) > \beta \ \ \forall x < T + \mu\} \\ &\leq P\{2D_n > \beta\}. \end{aligned}$$

In each case the probability converges to zero by the Glivenko–Cantelli lemma, which proves (ii). Note that since D_n converges with probability one, so does T_n. This in turn implies convergence in distribution.

To prove (iii) we need to show that the sequences $\{T_n\}$ and $\{T_n^2\}$ are uniformly integrable (for a proof, see [44]), i.e., that $\lim_{c\to\infty} \sup_n \int_c^\infty x g_{n,m,\varepsilon,f} dx = 0$ and that $\lim_{c\to\infty} \sup_n \int_c^\infty x^2 g_{n,m,\varepsilon,f} dx = 0$. We begin by bounding the density of T_n, $g_{n,m,\varepsilon,f}$, which we will abbreviate $g_n(x)$. In [30] we derived an explicit integral formula for $g_n(x)$. It is more convenient to write this expression in terms of the ordered inputs known as the order statistics. Let Y_i be the ith order statistic, i.e., the random variable which is the ith smallest of the X_i's. Let $f_{\{Y_i|T_n=Y_i\}}(x)$ denote the conditional density of Y_i given that $T_n = Y_i$, and let P_i be the probability that $T_n = Y_i$. The density $g_n(x)$ of T_n is the normalized sum from m to n of these conditional densities:

$$g_n(x) \ = \ \frac{\sum_{i=m}^n f_{\{Y_i|T_n=Y_i\}}(x) P_i}{P(\text{success})}. \tag{9}$$

Using the joint density of the Y_i's, we can compute $f_{\{Y_i|T_n=Y_i\}}(x)$ by integrating over the appropriate event:

$$\begin{aligned} &f_{\{Y_i|T_n=Y_i\}}(x) \\ &= \frac{1}{P_i} n! f(x) \int_{\Omega_3} \prod_{j=i+1}^{n} f(y_j) \int_{\Omega_2} \prod_{j=i-m+1}^{i-1} f(y_j) \int_{\Omega_1} \prod_{j=1}^{j=i-m} f(y_j) \prod_{j=1}^{i-1} dy_j \prod_{j=i+1}^{n} dy_j, \end{aligned} \tag{10}$$

where Ω_1, Ω_2, and Ω_3 are the sets

$$\begin{aligned} \Omega_1 &= \{y_1 < \cdots < y_{i-m} \ \text{ and } y_k < y_{k+m-1} - \varepsilon \text{ for } k = 1, \ldots, i-m\}, \\ \Omega_2 &= \{x - \varepsilon < y_{i-m+1} < \cdots < y_{i-1} < x\}, \\ \Omega_3 &= \{x < y_{i+1} < \cdots < y_n\}. \end{aligned}$$

The sets Ω_1, Ω_2, and Ω_3 correspond to the statements that the first $i-1$ arriving hits do not fire the cell, that the ith does, and that the remaining times can be anything.

We can attain a bound on the integral by replacing Ω_1 with the larger set

$$\Omega_1 = \{y_1 < \cdots < y_{i-m} \ \text{ and } y_{i-m} < x - \varepsilon\}.$$

Next we can integrate explicitly to obtain the bound on the conditional density

$$f_{\{Y_i|T_n=Y_i\}}(x) \leq \frac{1}{P_i} n! f(x) \frac{(1-F(x))^{n-i}}{(n-i)!} \frac{(F(x) - F(x-\varepsilon))^{m-1}}{(m-1)!} \frac{F(x-\varepsilon)^{i-m}}{(i-m)!}.$$

Summing over i in (9) gives the bound

$$g_n(x) \leq \frac{1}{P(\text{success})} n! \frac{(1-(F(x)-F(x-\varepsilon)))^{n-m}}{(n-m)!} \frac{(F(x)-F(x-\varepsilon))^{m-1}}{(m-1)!} f(x).$$

For large c, $F(x)-F(x-\varepsilon)$ goes to zero. We can make a straightforward calculation using Stirling's formula to show that $n! \frac{(1-(F(x)-F(x-\varepsilon)))^{n-m}}{(n-m)!} \frac{(F(x)-F(x-\varepsilon))^{m-1}}{(m-1)!}$ is uniformly bounded independent of n for $F(x)-F(x-\varepsilon)$ sufficiently small. Specifically if c is large enough so that $F(x)-F(x-\varepsilon) < \frac{a^a}{(a-1)^{a-1}}$ for all $x > c$, where a is the ratio n/m, then there is a constant A so that $g_n(x) \leq \frac{A}{P(\text{success})} f(x)$ for all $x > c$. Since f has a finite mean and standard deviation, this bound implies that $\{T_n\}$ and $\{T_n^2\}$ are both uniformly integrable, and so $E(T_n) \to T$ and $E(T_n^2) \to T^2$, which proves (iii).

Theorem 2.3 shows that if $F(x) - F(x-\varepsilon)$ crosses $\frac{m}{n}$ the first time it reaches $\frac{m}{n}$, then the firing time will converge to the point mass at this time as $n \to \infty$. The following two examples show that while most sets of parameters will be covered in the above theorems, we have not addressed what will happen if $F(x) - F(x-\varepsilon)$ is not increasing at T but rather reaches $\frac{m}{n}$ and is constant for some time or reaches $\frac{m}{n}$ and immediately drops back down. This situation is unlikely in the biological context but is of mathematical interest. Example 2.3 shows that if f is exponential, then either Theorem 2.2 or 2.3 will apply unless $F(x_o+\varepsilon)$ is exactly $\frac{m}{n}$. In Example 2.4 we discuss various cases in which the hypotheses of Theorem 2.3 are, or are not, satisfied.

Example 2.3. If f is exponential, then $F(x)-F(x-\varepsilon)$ will be monotone increasing from x_o to $x_o+\varepsilon$ and monotone decreasing for $x > x_o+\varepsilon$. If the value of $F(x)-F(x-\varepsilon)$ at its peak, namely $F(x_o+\varepsilon)$, is greater than $\frac{m}{n}$, then T will be less than ε and the hypotheses of Theorem 2.3 will be satisfied, so the standard deviation will go to zero (see Figure 3(A)). If, on the other hand, the value at the peak is less than $\frac{m}{n}$, then the set $\{x \,|\, F(x) - F(x-\varepsilon) \geq \frac{m}{n}\}$ is empty and the hypotheses of Theorem 2.2 will be satisfied, so the probability of firing will go to zero. It is of mathematical interest to study what will happen in the borderline case where $F(x_o+\varepsilon)$ is exactly $\frac{m}{n}$.

Example 2.4. Let $x_o < x_1 < y_o < y_1$ and suppose that the support of the density f consists of the two intervals $[x_o, x_1]$ and $[y_o, y_1]$. In addition, suppose that $x_1 - x_o < \varepsilon$, $y_1 - y_o < \varepsilon$, and $y_o - x_1 > \varepsilon$, so the intervals are small and well separated compared to ε. Let $p = \int_{x_o}^{x_1} f(x)\,dx$ and $q = \int_{y_o}^{y_1} f(x)\,dx$. There are several cases to consider. If $p > \frac{m}{n}$, then $x_o < T < x_1$ and the "strictly increasing" hypothesis holds, so the conclusions of Theorem 2.3 hold. If $p < \frac{m}{n}$ and $q < \frac{m}{n}$, then the probability of firing goes to zero as $n \to \infty$ with $\frac{m}{n}$ fixed by Theorem 2.2. If $p < \frac{m}{n}$ and $q > \frac{m}{n}$, then $y_o < T < y_1$ and again the "strictly increasing" hypothesis holds, so the conclusions of Theorem 2.3 hold. Finally, suppose that $\frac{m}{n} = \frac{1}{2}$ and that $p = q = \frac{1}{2}$. Then $T = x_1$ but the "strictly increasing" hypothesis does not hold. The number of hits in the first region is given by the binomial $B(n,p)$. Thus the probability of firing in this first interval, $P(B(n,p) \geq m)$, converges to $\frac{1}{2}$ as $n \to \infty$ with $\frac{m}{n}$ fixed. A straightforward argument shows that the conditional density (conditioned on firing in the first interval) converges to δ_{x_1}. The same arguments show that if the neuron does not fire in the first interval, then it has probability $\frac{1}{2}$ of firing in the second interval, and the conditional density (conditioned on firing in the second interval) converges to δ_{y_1}. Therefore, as $n \to \infty$ with $\frac{m}{n}$ fixed, the density (conditioned on firing) converges to $\frac{2}{3}\delta_{x_1} + \frac{1}{3}\delta_{y_1}$. Thus, if the "strictly increasing at T" hypothesis does not hold, the conclusions of Theorem 2.3 may not hold.

3. The asymptotic form. We will now prove the asymptotic normality of T_n. We will consider the case where, in addition to the left edge hypothesis (2) we assume that $T < x_0 + \varepsilon$. This means that there is more than m/n probability in the interval $(x_0, x_0 + \varepsilon)$, i.e., $F(x_o + \varepsilon) - F(x_o) > m/n$, and therefore that $F(x - \varepsilon) = 0$ for all $x < x_o + \varepsilon$.

THEOREM 3.1. *Suppose that $T < x_0 + \varepsilon$; then T_n is asymptotically normal with mean T and standard deviation*

$$\sigma_c = \frac{\left(\frac{m}{n}\left(1 - \frac{m}{n}\right)\right)^{1/2}}{f(T)n^{1/2}}. \tag{11}$$

We call the standard deviation σ_c because it is a result of the convergence studied in sections 1 and 2.

Proof. Fix t and let

$$G_n(t) = P\left(\frac{T_n - T}{\sigma_n} \leq t\right).$$

We wish to show that $G_n(t) \to \Phi(t)$, where Φ is the cumulative distribution for the standard normal. We begin by rewriting $G_n(t)$ using the definition of T_n given in (6):

$$\begin{aligned} G_n(t) &= P(T_n \leq T + t\sigma_n) \\ &= P\left(\exists x \leq T + t\sigma_n | F_n(x) - F_n(x - \varepsilon) \geq \frac{m}{n}\right). \end{aligned}$$

Since $\sigma_n \to 0$ as $n \to \infty$ and $T < x_0 + \varepsilon$, there is an $\bar{n}$ such that for all $n \geq \bar{n}$, $T + t\sigma_n < x_0 + \varepsilon$. Therefore if $n \geq \bar{n}$ and $x \leq T + t\sigma_n$, $F(x - \varepsilon) = 0$. Note that, by the definition of F_n, if $F(x - \varepsilon)$, then the probability of a hit before $x - \varepsilon$ is zero and $F_n(x - \varepsilon)$ is also zero for all n. So, for $n \geq \bar{n}$,

$$\begin{aligned} G_n(t) &= P\left(\exists x \leq T + t\sigma_n | F_n(x) \geq \frac{m}{n}\right) \\ &= P\left(F_n(T + t\sigma_n) \geq \frac{m}{n}\right), \end{aligned}$$

where we have used the monotonicity of F_n. Notice that since $F(T - \varepsilon) = 0$, the value T is just the value of the $\frac{m}{n}$th quantile, which we will denote ξ. The $\frac{m}{n}$th quantile is defined by $\xi = \inf\{x : F(x) \geq \frac{m}{n}\}$. The proof rests upon the asymptotic normality of the sample $\frac{m}{n}$th quantile, ξ_n, defined by $\xi_n = \inf\{x : F_n(x) \geq \frac{m}{n}\}$. ξ_n is asymptotically normal with mean ξ and standard deviation σ_n [44]. Now we can write G_n in terms of the quantiles:

$$G_n(t) = P(\xi_n \leq \xi + t\sigma_n).$$

Therefore the asymptotic normality of the sample quantile implies the asymptotic normality of T_n.

It is the hypothesis that $T < x_0 + \varepsilon$ that makes the proof of Theorem 3.1 easy by reducing the question to the asymptotic behavior of quantiles. Intuitively, the hypothesis means that there is a lot of probability close to the initial point x_0. Example 3.1 shows that this hypothesis is biologically reasonable. Example 3.2 shows what can happen if this hypothesis is violated and gives a conjecture for the general case.

Example 3.1. For neurons, the density f looks like AN (translated, smoothed) exponential [25, 51, 49] with standard deviation approximately 1 msec. In Figure 3(A)

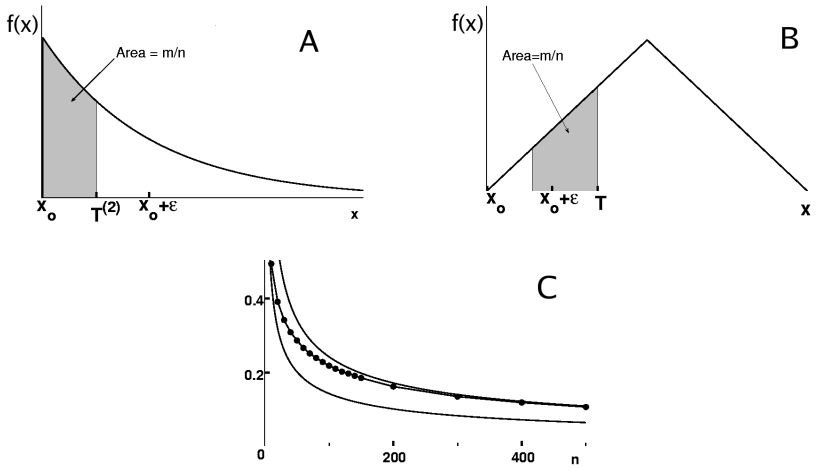

FIG. 3. *Examples illustrate the importance of the hypothesis* $T < x_o + \varepsilon$ *in Theorem* 3.1. *Panel* (A) *shows the density for the exponential as in Example* 3.1. *The shaded portion has area* $\frac{m}{n}$, *and one can see that* $T^{(2)} = x_o + \ln \frac{5}{3} < x_o + \varepsilon$ *so that Example* 3.1 *satisfies the hypotheses of Theorem* 3.1. *Similarly, the shaded portion in panel* (B) *has area* $\frac{m}{n}$, *but in this case* $T = 1.7 - \sqrt{6} > x_o + \varepsilon$ *so that Theorem* 3.1 *does not apply. Panel* (C) *compares results of Monte Carlo simulations (data are the dots on the middle curve) to the predictions of Theorem* 3.1, *(bottom curve,* σ_c*). We see that the theorem does not apply, but that our conjecture (top curve,* $\bar{\sigma}_c$*) for this more general case is supported.*

we show the exponential distribution (starting at x_0) with standard deviation 1 msec. It is easy to check that $T = x_0 + \ln \frac{n}{n-m}$. Consider three cases $\frac{m_1}{n_1} = .2$, $\frac{m_2}{n_2} = .4$, and $\frac{m_3}{n_3} = .5$, which will have corresponding $T^{(1)} = x_0 + \ln \frac{5}{4}$, $T^{(2)} = x_0 + \ln \frac{5}{3}$, and $T^{(3)} = x_0 + \ln 2$. Thus, if $\varepsilon = 1$ msec, which is reasonable for octopus cells [15, 32] and many other neurons, we will have $T^{(i)} < x_0 + \varepsilon$ in all three cases, so Theorem 3.1 applies.

Example 3.2. On the other hand, suppose that f is the piecewise linear "hat" distribution (see Figure 3(B)). In order to have standard deviation 1 msec, the density is supported on the interval $[-\sqrt{6}\sqrt{6}]$ (so $x_o = \sqrt{6}$). In all of the cases above $T^{(i)} > x_o + \varepsilon$, and so Theorem 3.1 does not apply. For example if $\frac{m}{n} = .2$, then $T = -\sqrt{6} + 1.7 \approx -0.75$. In this case the standard deviation does not converge to the value σ_c given in Theorem 3.1 but instead to another higher value. We conjecture that in this case T_n will be asymptotically normal with mean T and standard deviation

$$\bar{\sigma}_c = \frac{\left(\frac{m}{n}\left(1 - \frac{m}{n}\right)\right)^{1/2}}{(f(T) - f(T - \varepsilon))n^{1/2}}.$$

Figure 3(C) shows the values for σ_c (bottom curve), $\bar{\sigma}_c$ (top curve), and the standard deviation computed using Monte Carlo simulations as in [35] (middle curve; each dot was computed using 100,000 trials). We can see that for large n the values do not approach σ_c but rather $\bar{\sigma}_c$, supporting our conjecture.

4. Applications to octopus cells. The latency of a neuron in the auditory system is the length of time between the start of a sound and the time of the first action potential produced by the neuron. In mammals, AN neurons, which provide the

input to the auditory brainstem, have latencies in the range 2 to 8 msec, with standard deviations of approximately 1 msec under repeated trials [25]. The auditory system must use group properties of these highly variable inputs to extract sharp timing information so that the animal can make time distinctions in the low microsecond range. According to Oertel et al. [32], much of this processing is done by octopus cells in the cochlear nucleus that "detect coincident firing within populations of auditory nerve fibers and convey acoustic information in precisely timed action potentials." It is estimated that octopus cells receive synapses from roughly 60 to 100 AN neurons (i.e., $60 \leq n \leq 100$) and require that 20% to 50% of these synapses be activated by incoming action potentials within 1 msec in order fire an action potential (i.e., $\varepsilon =$ 1 msec and $0.2 \leq \frac{m}{n} \leq 0.5$) [32, 15]. It is therefore of interest to test whether the predictions of the theorems in this paper are consistent with the observed in vivo and in vitro behavior of octopus cells. For some parameter choices we can also make more specific predictions for optimal values of m and n.

The histograms of latencies in AN neurons are quite variable but look roughly like smoothed exponential distributions. Thus, we shall assume that f is exponential with standard deviation 1 msec, and it follows that $T = x_o + \log \frac{n}{n-m}$. If $\varepsilon \geq T$, which holds for all cases considered below (see Example 3.1 above), then $F(T-\varepsilon) = 0$, and the asymptotic formula (11) has the simple form

$$\sigma_c^2 \;=\; \frac{\frac{m}{n}}{(1-\frac{m}{n})n}. \tag{12}$$

If we evaluate σ_c for n and m in the physiological ranges given above, we obtain values in the range 0.05 msec to 0.13 msec (Table 2). Oertel et al. report that the standard deviations of latencies of octopus cells in response to sounds are approximately 0.1 msec [32], so the formula (11) certainly predicts the order of magnitude improvement of timing seen in vivo in octopus cells.

We can use (12) to explore a variety of questions about the physiology of octopus cells. First we ask why n isn't larger than the range 60–100. σ_c is the standard deviation in the latency of the octopus cell due to the variation in firing times of the inputs. However, there are other sources of variation. The AN neurons that synapse on the octopus cell may have somewhat different axonal lengths and diameters, both of which will affect arrival times. Second, due to such factors as the diffusion of neurotransmitter across the synaptic cleft, the finite number of postsynaptic receptors, and the variation in the local membrane chemistry, the integration of synaptic inputs by the octopus cell will have variation under repeated trials even if the timing of the inputs is the same. Assuming that these other factors are independent of the noise in the firing times of the inputs, and denoting the corresponding standard deviation by σ_{other}, we have $\sigma_o^2 = \sigma_c^2 + \sigma_{other}^2$. Fortunately, the experiments in [15], where shocks are applied to the nerve root, give a good estimate, $\sigma_{other} = 0.05$ msec. Figure 3 shows the behavior of σ_o as a function of n in two cases, $\frac{m}{n} = \frac{1}{2}$ and $\frac{m}{n} = \frac{1}{5}$, that are

TABLE 2
Values of σ_c.

n	m	σ_c (msec)
100	20	0.05
100	33	0.07
100	50	0.10
60	30	0.13

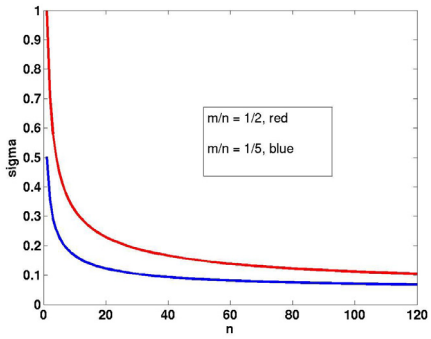

FIG. 4. *Predicted values of the standard deviation of the latency of octopus cells, σ_o, for different values of n.*

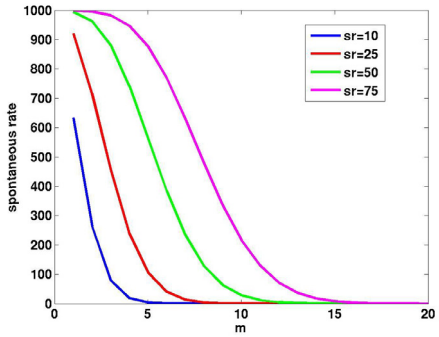

FIG. 5. *Predicted values of the spontaneous rate of the octopus cell as a function of m with $n = 100$ and four different assumptions about the spontaneous rate, r, of AN neurons.*

the expected extremes for the ratio $\frac{m}{n}$. In both cases there is not much extra decrease in σ_o after $n = 60$ and very little after $n = 100$.

Many AN neurons have high or very high spontaneous rates, even ranging as high as 100 spikes/sec [25, 19]. If n is high and m is low, then many of the successful firings of the octopus cell will be spontaneous, i.e., unrelated to input. However, it is known that octopus cells have essentially no spontaneous rate [37, 38, 46]. Thus, it is a natural question to ask how large m must be so that the spontaneous rate of the octopus cell in our model is 1 spike/sec or less. Assume $\varepsilon = 1$ msec, and suppose that each incoming AN neuron has a spontaneous rate of r spikes/msec. Then, the probability that any particular AN neuron delivers a spike within a 1 msec interval is approximately r. Assuming that the AN neurons are independent, the probability of m or more incoming spikes within the 1 msec interval is approximately

$$Prob\{\#\text{incoming hits} \geq m\} = \sum_{k=m}^{n} \binom{n}{k} r^k (1-r)^{n-k}, \tag{13}$$

and thus the spontaneous firing rate of the octopus cell in spikes/sec, denoted by $SR(r, n, m)$, will be approximately 1000 times the probability in (13). Figure 5 shows the graphs of $SR(r, n, m)$ as functions of m for $n = 100$ and for four different choices of r. If the incoming AN fibers have spontaneous rates of $r = .075$ spikes/msec

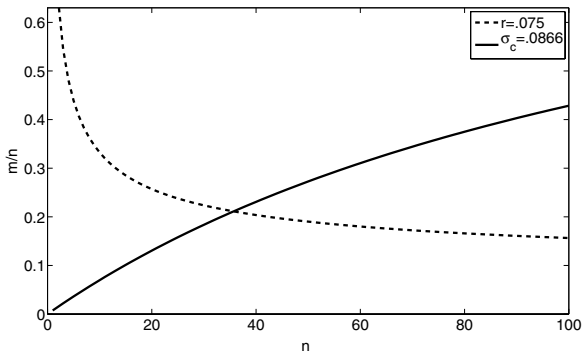

FIG. 6. *The region of the* $(\frac{m}{n}, n)$ *plane for which* $\sigma_o \leq 0.1$ *and the octopus cell has a spontaneous firing rate* ≤ 1 *spike/sec is the region below the solid curve and above the dashed curve.*

(75 spikes/sec), $SR(.075, 100, m)$ does not go below 1 spike/sec until $m = 18$. Thus the model, with $n = 100$, predicts that m is 18 or higher, which corresponds well with the estimates of experimentalists [15, 32, 13].

We can also allow both $\frac{m}{n}$ and n to be free and ask what is the region in the $(n, \frac{m}{n})$ plane that gives the observed physiological behavior. First, we require that the standard deviation of the latency of the octopus cell satisfy $\sigma_o \leq 0.1$ msec. Since $\sigma_o^2 = \sigma_c^2 + \sigma_{other}^2$, this is equivalent to the requirement that $\sigma_c^2 \leq .1^2 - .05^2$. Equation (12) can be rearranged to give a bound on $\frac{m}{n}$ in terms of this maximum allowable standard deviation:

$$\frac{m}{n} \leq \frac{(\sigma_c^2)n}{1 + (\sigma_c^2)n}. \tag{14}$$

Second, we require that the spontaneous firing rate of the octopus cell be less than the maximum value $r_{max} = .001$ spike/msec or 1 spike/sec. Using (13) and the normal approximation to the binomial gives

$$\frac{m}{n} \geq \Phi^{-1}(1 - r_{max})\sqrt{\frac{r(1-r)}{n}} + r, \tag{15}$$

where Φ is the cumulative distribution function of the standard normal and r is the spontaneous rate of the incoming neurons. The points below the solid curve in Figure 6 satisfy (14), and the points above the dashed curve satisfy (15) in the case $r = .075$ spikes/msec.

In Figure 6 we assumed that the standard deviation of f is 1 msec and that the spontaneous rate of the AN neurons $r = 75$spikes/sec. For other assumptions the curves are somewhat different. For example, instead of choosing $\sigma_c = .0866$, we could recognize that it is not particularly beneficial to require that σ_c be smaller than σ_{other}. In this case we require that σ_c be roughly the same as σ_{other} so that both are equal to .05 msec and repeat the above calculations (shown in Figure 7), predicting a much smaller region of possible values for m and n. In this case we require $n \geq 80$ and that $\frac{m}{n}$ be between 18% and 20%. This is within the experimental estimates but suggests a much smaller range of optimal values. From this calculation we can predict that ideally n should be near the high end of its range, close to 100, and that m should be near the low end of its range, close to 20.

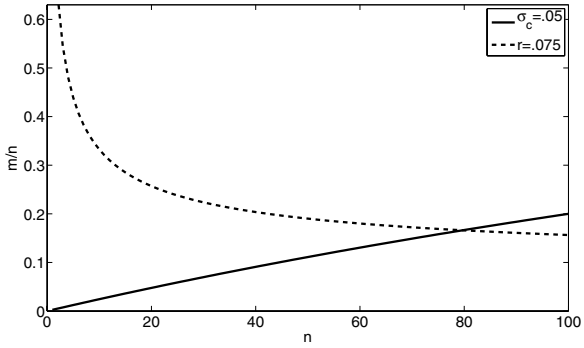

FIG. 7. *The region of the* $(\frac{m}{n}, n)$ *plane for which* $\sigma_c \leq 0.05$ *and the octopus cell has a spontaneous firing rate* ≤ 1 *spike/sec is the region below the solid curve and above the dashed curve. In both Figures* 6 *and* 7*, we assume that the standard deviation of* f *is* 1 *msec and that the spontaneous rate of the AN neurons* $r = 75$ *spikes/sec.*

5. Discussion. The model given in Figure 1 was formulated to allow a mathematical investigation of how convergence (the number of incoming neurons, n) and the number of hits required to make the target cell fire, m, affect the sharpening of timing information when the firing times of the incoming neurons are noisy. The main theorem (Theorem 2.3) shows that if $n \to \infty$ and $m \to \infty$ with $\frac{m}{n}$ fixed, then the standard deviation of the time of firing of the target cell goes to zero. The physiological significance of the result is that timing can be sharpened by taking both n large and m large (to avoid spontaneous firing of the target). That there should be a theorem like this was suggested by the approximate calculations of Burkitt and Clark [4] and the numerical simulations of Kalluri and Delgutte [23]. In section 3 we derived approximate formulas for $g_{n,m,\varepsilon,f}$ and $\sigma_{n,m,\varepsilon,f}$ near the limit. In section 4, we used the asymptotic formula for $\sigma_{n,m,\varepsilon,f}$ to study octopus cells of the mammalian cochlear nucleus and saw that the predictions of the mathematical model correspond quite well to experimental observations.

We hope that the theorems proved in this paper can be a first step in proving theorems about more complicated and difficult neurophysiological questions. One such question is the improved phase locking of CN neurons compared to the phase locking in the AN [19, 22, 43, 4, 23], which is universally believed to occur because of convergence of many AN fibers on CN target cells. The mathematical situation here is more complicated, since typically one models the firing pattern in individual AN fibers by a Poisson process whose parameter $\lambda(t)$ depends on the sound; for example, $\lambda(t)$ would be periodic for a pure tone. The quantity of interest is the distribution of spike times of the target cell modulo the nearest multiple of the period. For some cells the target cell may fire at first hit, while for other cells many subthreshold hits in a small time window may be necessary for firing. Because of the background noise caused by the high spontaneous rates of many AN fibers, this may be an excellent use of the theory of stochastic resonance [17, 47]. To prove such theorems one would need to represent the noise as stochastic processes rather than making the simple approximations that we have used in section 4. Another such question is how synchronous firing of large groups of neurons in the CNS is created and maintained. Such firing has been proposed as central to "binding" mechanisms in the visual system [12, 26, 28], the improvement of coordination of motor systems in the cerebellum [20], and the creation of the γ

rhythm [3]. The approximation theorem in section 3 is a natural starting point for studying synfire chains [1, 11, 36, 18] that have both noise and high convergence from level to level. Many of the models for these systems involve inhibition, so an important step would be the extension of the results in [35, 30] and this paper to include inhibitory neurons.

In applying our model to octopus cells we have simplified the biological situation in several ways. First, AN neurons synapse serially on the large dendrites of octopus cells, not directly on the cell body as in our model. Oertel has shown [32] that the AN neurons that carry higher frequency sounds (they fire on average earlier) synapse further out on the dendrite, and the AN neurons that carry lower frequency sounds (they fire on average later) synapse closer to the cell body. Golding, Ferragamo, and Oertel [16] conclude that this arrangement on the dendrite, as well as the thickness of the dendrite and special channel properties, insure that the influence of each AN neuron arrives (on average) at the cell body at the same time, which justifies our assumption that all the AN neurons synapse directly on the cell body.

A much more serious simplification is that we have ignored the detailed biophysics of synapses and the postsynaptic membrane. All the biophysics is contained in the two parameters, ε, the time window, and m, the number of hits required in that time window to fire the target cell. We believe that the results in section 4 show conclusively that our model, with these two simple parameters, explains why octopus cells improve the standard deviation of timing by one order of magnitude and why octopus cells have no spontaneous rates. Of course, the *values* of these two parameters arise from the detailed biophysics of the synapses and postsynaptic membrane.

Finally, it is reasonable to ask whether octopus cells, or indeed any neurons, have sharp time windows as we assume in our model. Ferragamo and Oertel [13] have conducted a detailed study of the potential of the postsynaptic membrane of octopus cells. They showed that it is the rate of rise of the potential (dependent on the rate of arrival of incoming spikes) that determines whether the octopus cell fires. This is exactly what one would expect if the octopus cell had a sharp time window. If the rate of rise is high enough, then there will be enough incoming spikes in the time window, and if the rate of rise is too slow, then there will not be enough incoming spikes in the time window. More generally, we have studied a number of frequently used non-linear models for the biophysics of postsynaptic membranes and have shown that, in reasonable parameter ranges, they have quite sharp time windows. These results will appear in a subsequent publication [31].

Acknowledgments. The authors are very grateful to Professor Donata Oertel, who raised many of the questions discussed in section 4. We would also like to thank Matthew Moehlmann, who wrote the code for the Monte Carlo simulation in Example 3.2.

REFERENCES

[1] M. Abeles, *Corticonics: Neural Circuits of the Cerebral Cortex*, Cambridge University Press, Cambridge, UK, 1991.
[2] P. Billingsley, *Probability and Measure*, Wiley, New York, 1975.
[3] C. E. Borgers and N. Kopell, *Synchronization in networks of excitatory and inhibitory neurons with sparse, random connectivity*, Neural Comput., 15 (2003), pp. 509–538.
[4] A. Burkitt and G. Clark, *Analysis of integrate-and-fire neurons: Synchronization of synaptic input and spike output*, Neural Comput., 11 (1999), pp. 871–901.
[5] A. Burkitt and G. Clark, *Synchronization of the neural response to noisy periodic synaptic input*, Neural Comput., 13 (2001), pp. 2639–2672.

[6] Y. Cai, E. Walsh, and J. McGee, *Mechanisms of onset responses in octopus cells of the cochlear nucleus: Implications of a model*, J. Neurophysiol., 78 (1997), pp. 872–883.
[7] Y. Cai, J. McGee, and E. Walsh, *Contributions of ion conductances to the onset responses of octopus cells in the ventral cochlear nucleus: Simulation results*, J. Neurophysiol., 83 (2000), pp. 301–314.
[8] H. Colburn, *Theory of binaural interaction based on auditory-nerve data.* I. *General strategy and preliminary results on interaural discrimination*, J. Acoust. Soc. Amer., 54 (1973), pp. 1458–1470.
[9] H. Colburn, *Theory of binaural interaction based on auditory-nerve data.* II. *Detection of tones in noise*, J. Acoust. Soc. Amer., 61 (1977), pp. 525–533.
[10] E. Covey and J. H. Casseday, *The monaural nuclei of the lateral lemniscus of the echolocating bat: Parallel pathways for analyzing the temporal features of sounds*, J. Neurosci., 11 (1991), pp. 3456–3470.
[11] M. Diesmann, M.-O. Gewaltig, S. Rotter, and A. Aersted, *Stable propagation of synchronous spiking in cortical neural networks*, Nature, 402 (1999), pp. 529–533.
[12] A. K. Engel, P. Konig, and W. Singer, *Direct physiological evidence for scene segmentation by temporal coding*, Proc. Natl. Acad. Sci. USA, 88 (1991), pp. 9136–9140.
[13] M. Ferragamo and D. Oertel, *Octopus cells of the mammalian cochlear nucleus sense the dynamic properties of synaptic excitation*, J. Neurophysiol., 87 (2003), pp. 2262–2270.
[14] J. M. Goldberg and P. B. Brown, *Response of binaural neurons of dog superior olivary complex to dichotic tone stimuli: Some physiological mechanisms of sound localization*, J. Neurophysiol., 32 (1969), pp. 613–636.
[15] N. Golding, D. Robertson, and D. Oertel, *Recordings from slices indicate that octopus cells of the cochlear nucleus detect coincident firing of auditory nerve fibers with temporal precision*, J. Neurosci., 15 (1995), pp. 3138–3153.
[16] N. Golding, M. Ferragamo, and D. Oertel, *Role of intrinsic conductances underlying responses to transients in octopus cells of the cochlear nucleus*, J. Neurosci., 19 (1999), pp. 2897–2905.
[17] P. E. Greenwood, U. U. Muller, L. M. Ward, and W. Wefelmeyer, *Statistical analysis of stochastic resonance in a thresholded detector*, Aust. J. Stat., 32 (2003), pp. 49–70.
[18] G. Hayon, M. Abeles, and D. Lehmann, *A model for representing the dynamics of a system of synfire chains*, J. Comput. Neurosci., 18 (2005), pp. 41–53.
[19] D. R. F. Irvine, *The Auditory Brainstem*, Springer-Verlag, New York, 1986.
[20] R. Ivry, *Cerebellar timing systems*, Internat. Rev. Neurobiol., 41 (1997), pp. 555–573.
[21] L. A. Jeffress, *A place theory of sound localization*, J. Comput. Psychol., 41 (1947), pp. 35–39.
[22] P. X. Joris, L. H. Carney, P. H. Smith, and T. Yin, *Enhancement of neural synchronization in the anteroventral cochlear nucleus.* I. *Responses to tones at the characteristic frequency*, J. Acoust. Soc. Amer., 71 (1994), pp. 1022–1036.
[23] S. Kalluri and B. Delgutte, *Mathematical models of cochlear onset neurons:* I. *Point neuron with many synaptic inputs*, J. Comput. Neurosci., 14 (2003), pp. 71–90.
[24] S. Kalluri and B. Delgutte, *Mathematical models of cochlear onset neurons:* II. *Model with dynamic spike-blocking state*, J. Comput. Neurosci., 14 (2003), pp. 91–110.
[25] N. Kiang, *Discharge Patterns of Single Fibers in the Cat's Auditory Nerve*, MIT Press, Cambridge, MA, 1996.
[26] P. Konig, A. K. Engel, and W. Singer, *Integrator or coincidence detector? The role of cortical neurons revisited*, Trends. Neurosci., 19 (1996), pp. 130–137.
[27] P. Marsalek, C. Koch, and J. Maunsell, *On the relationship between synaptic input and spike output jitter in individual neurons*, Proc. Natl. Acad. Sci. USA, (1997), pp. 735–740.
[28] M. S. Matell and W. H. Meck, *Neurophysiological mechanisms of interval timing behavior*, BioEssays, 22 (2000), pp. 94–103.
[29] C. Mitchell, *Mathematical Properties of Time-Windowing in Neural Systems*, thesis, Duke University, Durham, NC, 2003.
[30] C. Mitchell, *Precision of neural timing: The small ε limit*, J. Math. Anal. Appl., 309 (2005), pp. 567–582.
[31] C. Mitchell and M. Reed, *Mathematical Properties of Time-Windowing in Neural Systems, Emergent Time Windows in Nonlinear Neural Models*, in preparation, 2007.
[32] D. Oertel, R. Bal, S. Gardner, P. Smith, and P. Joris, *Detection of synchrony in the activity of auditory nerve fibers by octopus cells of the mammalian cochlear nucleus*, Proc. Natl. Acad. Sci. USA, 97 (2000), pp. 11773–11779.
[33] G. D. Pollak, *Some comments on the perception of phase and nanosecond time disparities by echolocating bats*, J. Comput. Physiol. A, 172 (1993), pp. 523–531.

[34] L. Rayleigh (J. W. Strutt), *On our perception of sound direction*, Phil. Mag., 13 (1907), pp. 214–232.
[35] M. Reed, J. Blum, and C. Mitchell, *Precision of neural timing: Effects of convergence and time-windowing*, J. Comput. Neurosci., 13 (2002), pp. 35–47.
[36] A. Reyes, *Synchrony-dependent propagation of firing rate in iteratively constructed networks* in vitro, Nature Neurosci., 6 (2003), pp. 593–599.
[37] W. S. Rhode, D. Oertel, and P. H. Smith, *Physiological response properties of cells labelled intracellularly with horseradish peroxidase in cat ventral cochlear nucleus*, J. Comput. Neurol., 213 (1983), pp. 448–463.
[38] W. S. Rhode and P. H. Smith, *Encoding timing and intensity in the ventral cochlear nucleus of the cat*, J. Neurophysiol., 56 (1986), pp. 261–286.
[39] J. S. Rothman and P. B. Manis, *Differential expression of three distinct potassium currents in the ventral cochlear nucleus*, J. Neurophysiol., 89 (2003), pp. 3070–3082.
[40] J. S. Rothman and P. B. Manis, *Kinetic analyses of three distinct potassium conductances in ventral cochlear nucleus neurons*, J. Neurophysiol., 89 (2003), pp. 3083–3096.
[41] J. S. Rothman and P. B. Manis, *The roles potassium currents play in regulating the electrical activity of ventral cochlear nucleus neurons*, J. Neurophysiol., 89 (2003), pp. 3097–3113.
[42] J. Rothman, E. Young, and P. Manis, *Convergence of auditory nerve fibers onto bushy cells in the ventral cochlear nucleus: Implications of a computational model*, J. Neurophysiol., 70 (1993), pp. 2562–2582.
[43] J. Rothman and E. Young, *Enhancement of neural synchronization in computational models of ventral cochlear nucleus bushy cells*, J. Auditory Neurosci., 2 (1996), pp. 47–62.
[44] R. Serfling, *Approximation Theorems of Mathematics Statistics*, Wiley, New York, 1976.
[45] J. A. Simmons, M. Ferragamo, C. F. Moss, S. B. Stevenson, and R. A. Altes, *Discrimination of jittered sonar echoes by the echolocating bat,* Eptesicus fuscus*: The shape of target images in echolocation*, J. Comput. Physiol. A, 167 (1990), pp. 589–616.
[46] P. H. Smith, P. X. Joris, M. I. Banks, and T. Yin, *Responses of cochlear nucleus cells and projections of their axons*, in The Mammalian Cochlear Nuclei: Organization and Function, M. A. Merchan, J. M. Juiz, D. A. Godfrey, and E. Mugnaini, eds., Plenum, New York, 1993, pp. 349–360.
[47] M. Stemmler, *A single spike suffices: The simplest form of stochastic resonance in model neurons*, Computation in Neural Systems, 7 (1996), pp. 687–716.
[48] G. Svirskis, V. Kotak, D. Sanes, and J. Rinzel, *Enhancement of signal-to-noise ratio and phase locking for small inputs by a low threshold outward current in auditory neurons*, J. Neurosci., 22 (2002), pp. 11019–11025.
[49] T. Yin, *personal communication.*
[50] W. Yost and G. Gourevitch, eds., *Directional Hearing*, Springer-Verlag, New York, 1987.
[51] E. Young, J.-M. Robert, and W. Schofner, *Regularity and latency of units in ventral cochlear nucleus: Implications for unit classification and generation of response properties*, J. Neurophysiol., 60 (1988), pp. 1–29.